A Novel Bonding Method of Pure Aluminum and SUS304 Stainless Steel Using Barrel Nitriding

JUNG HYUN KONG, MASAHIRO OKUMIYA, YOSHIKI TSUNEKAWA, KY YOUL YUN, SANG GWEON KIM, and MASASHI YOSHIDA

A great deal of research is being carried out on welding or bonding methods between iron and aluminum. However, it is not so easy to make Fe-Al bonding materials with both high strength and light weight. Recently, a new nitriding process has been proposed to produce aluminum nitride on an aluminum surface using a barrel. This study proposes a new concept in the production of a multilayer which has an AlN and Fe-Al intermetallic compound layer between the aluminum and steel using a barrel nitriding process. The bonding process was carried out from 893 K to 913 K (620 °C to 640 °C) for 18, 25.2, and 36 ks with Al_2O_3 powder and Al-Mg alloy powder. After the process, an aluminum nitride (AlN) layer and a Fe-Al intermetallic compound ($Fe_2Al_{5.4}$) layer were formed at the interface between the pure aluminum and SUS304 austenitic stainless steel. The thicknesses of the AlN layer and the intermetallic compound layer increased with increasing treatment temperature and time. The maximum hardnesses of the AlN layer and $Fe_2Al_{5.4}$ layers were found to be 377HV and 910HV, respectively, after barrel nitriding at 893 K (620 °C) for 18 ks.

I. INTRODUCTION

AUTOMOTIVE and aerospace industries have increasingly employed aluminum (Al) and Al alloys in manufacturing due to their light weight, high specific strength, good machinability, formability, and corrosion resistance compared to most steels.[1,2] With the increasing use of aluminum alloys to help reduce the vehicle weight and improve fuel efficiency,[3,4] there is an increasing need for dissimilar metal joining of Al to steel, which is still widely used in vehicles. It has been suggested that the joint between Al and steel can combine the advantages of the two materials and can have broad application prospects in the automotive, aerospace, shipbuilding, and other industries.[5–7]

Most joining methods are preceded by brazing or welding process. For example, solid-state welding, such as friction welding, friction stir welding, roll welding, and ultrasonic welding, is used to weld Al to steel. These methods can produce high-quality joints,[8–13] but are often limited to special workpiece geometry, workpiece dimensions, joint designs, backing, etc. In addition,

these methods are generally accompanied by the degradation of the properties of the materials in the melting zone.

Joining Al to steel is a great challenge because of the large differences in thermo-physical properties between the two materials,[14] and especially because of the strong tendency to form Fe-Al intermetallic compounds at elevated temperatures. The large differences between Al and steel in thermo-physical properties, such as melting point, thermal conductivity, and thermal expansion coefficient, can lead to high residual stresses in the resultant welds.

In recent years, a new nitriding method using a barrel has been reported, which has the effect of the physical polishing of the surface for forming a nitride layer after the removal of the natural oxide film of aluminum.[15] In addition, a multilayer of AlN and Fe-Al could be formed at the interface between the aluminum and steel after barrel nitriding.[16] As is well known, AlN and Fe-Al intermetallic compounds are regarded as promising materials for industrial applications because of their excellent corrosion resistance, high wear resistance, and specific strength with high hardness values and high temperature strength.[17–22]

It is expected that through this new bonding method using barrel process, it is possible to apply the bonding process of steel and aluminum without the degradation of substrates and to keep the bonding strength. It replaces some automobile and the aircraft parts with a high-strength light metal. This, therefore, leads to an increase in the efficiency of the mode of transportation and reduces consumption in resources and energy. It is the realizable way of the Negawatt.[23] In addition, most of diffusion bonding process was conducted at a constant pressure and temperature with a filler metal

JUNG HYUN KONG, Postdoctoral Fellow, and MASAHIRO OKUMIYA and YOSHIKI TSUNEKAWA, Professors, are with the Toyota Technological Institute, 2-12-1, Hisakata, Tempaku, Nagoya 468-8511, Japan. Contact e-mail: kongja83@toyota-ti.ac.jp; kongja83 @gmail.com KY YOUL YUN, Assistant Professor, is with the Faculty of Engineering and Graduate School of Engineering, Gifu University, Gifu 501-1193, Japan. SANG GWEON KIM, Researcher, is with the Surface Technology & Heat Treatment R&D Department, Korea Institute of Industrial Technology 7-47, Songdo-Dong, Yeonsu-Gu, Incheon 406-840, South Korea. MASASHI YOSHIDA, Professor, is with the Department of Mechanical Engineering, Shizuoka Institute of Science and Technology, Hukuroi 437-8555, Japan.

at the interface.[24] Moreover, it is well known that the diffusion bonding of aluminum and stainless steel is very difficult; in addition, there are no reports on the formation of multilayer at the interface between aluminum and stainless steel at the same time. In this paper, the formation of a multilayer which has an aluminum nitride (AlN) and Fe-Al bonding layer was investigated between pure aluminum and SUS304 stainless steel, which was produced using the barrel nitriding process.

II. EXPERIMENTAL PROCEDURES

A. Specimen Preparation

JIS-A1050 commercial grade pure aluminum was used as a substrate material, with a size of 20 mm width × 50 mm length × 3 mm thickness. In addition, SUS304 austenitic stainless steel was prepared and machined to the same size as the pure Al for the bonding process. The specimens were fixed by stainless steel wire (0.4Φ) after grinding on the #200 emery paper. The specific chemical compositions measured by a spectrometer (Ametek., Spectrolab) and the results are shown in Table I.

B. Bonding Process (Barrel Nitriding)

Al_2O_3 powder (average diameter 0.1 mm) and Al 50 wt pct Mg alloy powder (average diameter 0.2 mm) was prepared as filler for the inside of the barrel chamber. The furnace was evacuated by a rotary pump, and the pressure was maintained at 7.5×10^{-1} torr before the treatment; after that, the atmosphere was substituted by N_2 gas up to 1.1 kgf/cm^2, while the temperature is raised to a target temperature. Since the nitrogen gas pressure is sufficiently applied in the barrel chamber, the nitrogen gas just flow with the 1500 cc/min. The N_2 gas flow rate was adjusted with a program control unit and a mass flow controller. The furnace temperature was adjusted with a temperature control unit. A schematic diagram of the barrel nitriding furnace used for the experiment is shown in Figure 1.

After the introduction of N_2, barrel nitriding was carried out with the oscillation of the barrel chamber at the temperature range of 893 K to 913 K (620 °C to 640 °C) for 10.8, 18, 25.2, and 36 ks. After a holding time, the specimen was cooled in the barrel. The temperature inside of the powder was measured by a thermocouple; the temperature and the N_2 gas flow rate were both monitored with a data processor. The parameters of the barrel nitriding process are shown in Table II.

C. Micro-structure Observation

The optical microscopy (OM), scanning electron microscopy (SEM-EDX), (HITACHI, SU6600) and electron probe micro analyzer (EPMA) (JEOL, JXA-8230) were used to observe the micro-structure and morphology after grinding and polishing on the cross section of bonded specimens. The structures of the AlN and Fe-Al intermetallic compound layers were identified by an X-ray diffractometer (Rigaku, UltraX 18TTR) using monochromatic Cu K_α radiation. The X-ray diffraction (XRD) measurements were performed using a goniometer at a scanning range of 30 deg $\leq 2\theta \leq$ 80 deg at 40 kV and 200 mA with a step size of 0.02 deg. The Al substrate was mechanically polished to the AlN and Fe-Al intermetallic compound layer in regular increments in order to measure the XRD for each layer.
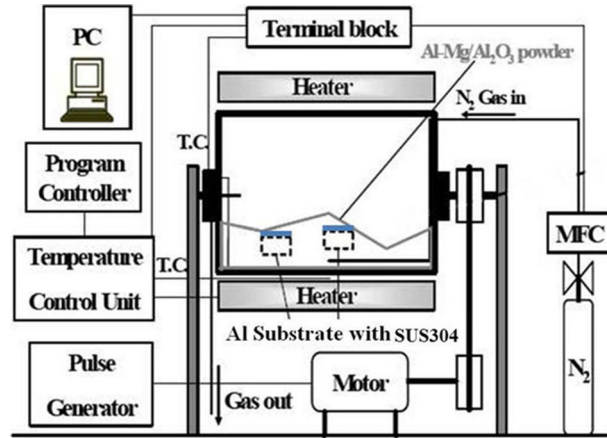

Fig. 1—A schematic diagram of the bonding (barrel nitriding) process.

Table II. Treatment Condition of Barrel Nitriding

Barrel Nitriding	
Nitriding temperature T [K (°C)]	883, 893, 903 and 913 (610, 620, 630 and 640)
Heating time (ks)	5.4
Nitriding time (ks)	10.8, 18, 25.2, 36 and 172.8
Nitriding gas	nitrogen (N_2)
Nitrogen gas flow (cc/min)	1,500
Filler	Al_2O_3 (average dia. 0.1 mm) Al-50 wt pct Mg (average dia. 0.2 mm)
Al-Mg/Al_2O_3 ratio (wt pct)	1.6

Table I. Chemical Compositions of A1050 and SUS304

Specimen	Si	Fe	Cu	Mn	Mg	Zn	Ti	Al
A1050	0.0951	0.318	0.014	0.0028	0.0041	0.0038	0.0138	bal.

Specimen	C	Si	Mn	P	S	Ni	Cr	Fe
SUS304	0.0395	0.515	0.908	0.0172	0.0041	7.24	19.20	bal.

D. *Measurement of Hardness*

The micro-hardness of the AlN and Fe-Al intermetallic compound layer was measured by a Vickers micro hardness tester (Akashi, HM-125). The hardness measurements were performed from the Al substrate to the SUS304 stainless steel with the AlN and Fe-Al intermetallic compound layer under a load of $200 \times g$ for 10 seconds on the cross-sectional region.

III. RESULTS AND DISCUSSION

Figure 2 shows the optical micrographs of multilayers which were formed between the pure aluminum (JIS A1050) and SUS304 austenitic stainless steel after barrel nitriding at 893 K (620 °C) for 10.8, 18, 25.2, and 36 ks.

After treatment, multilayers are formed between pure aluminum and SUS304 at 893 K (620 °C) for 10.8 to 36 ks, and the thickness is increased with increasing treatment time. However, the multilayer is not formed fully at 893 K (620 °C) for 10.8 ks. It is apparent that the treatment time of 10.8 ks is not enough for forming the multilayer. That is, it is decided that the thin oxide film on aluminum surface is not broken completely at this treatment temperature and time. The total thickness of the multilayer was found to be 115, 160, 180, and 300 μm at each treatment time. Generally, it has been known that Al atoms have a strong affinity with nitrogen atoms. In addition, aluminum nitride can be formed with aluminum under 933 K (660 °C), as shown in Figure 3(a).[25] At the results of the EPMA analysis of the cross section (Figure 4), the multilayer is composed of aluminum nitride layer and Fe-Al intermetallic compound layer. The layers were produced by the diffusion of nitrogen and aluminum, respectively.

Figure 3(b) is the Fe-Al phase diagram[26] which shows five types of Fe-Al intermetallic compounds. It has been known that the $FeAl_2$, Fe_2Al_5, and $FeAl_3$ compounds which have a high aluminum composition have high hardness values with brittleness.

In addition, Fe_3Al and FeAl compounds also have good mechanical properties in the aspects of wear resistance, oxidation resistance, corrosion resistance, and specific strength properties.[5] Therefore, the compound layer can be expected to act as a reinforcement which has a strong impact resistance due to the high strength and high hardness of the multilayer even though the bonded materials have a light weight.

Figure 5 shows the cross-sectional optical micrographs of the bonded multilayers which were formed between the pure Al and SUS304 austenitic stainless steel at the temperatures of 893 K, 903 K, and 913 K (620 °C, 630 °C, and 640 °C) for various treatment times. As shown in Figure 5, the multilayers are composed of aluminum nitride layer (A) and Fe-Al intermetallic layer (B). The total thickness of the multilayer increased with increasing treatment time and temperature. In particular, the thickness of the nitride layer is greater than that of the Fe-Al intermetallic
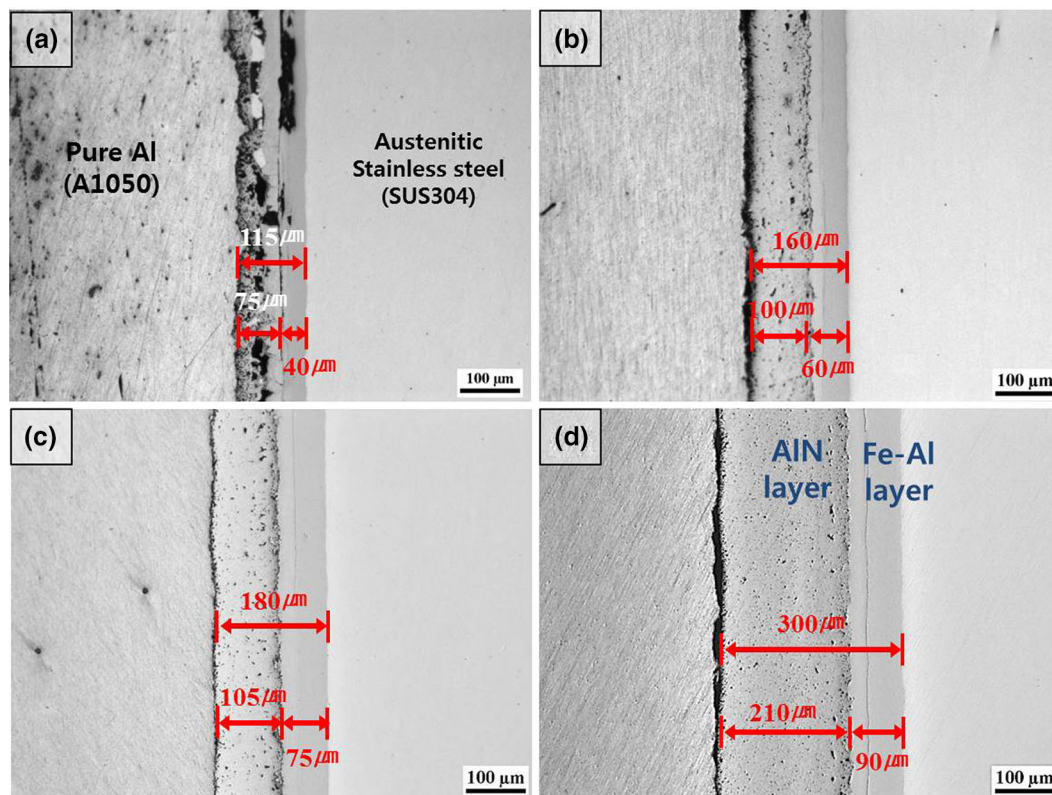

Fig. 2—Cross-sectional micrographs of the multilayer between the pure aluminum and SUS304 stainless steel after bonding process at 893 K (620 °C) for (*a*) 10.8 ks, (*b*) 18 ks, (*c*) 25.2 ks, and (*d*) 36 ks.
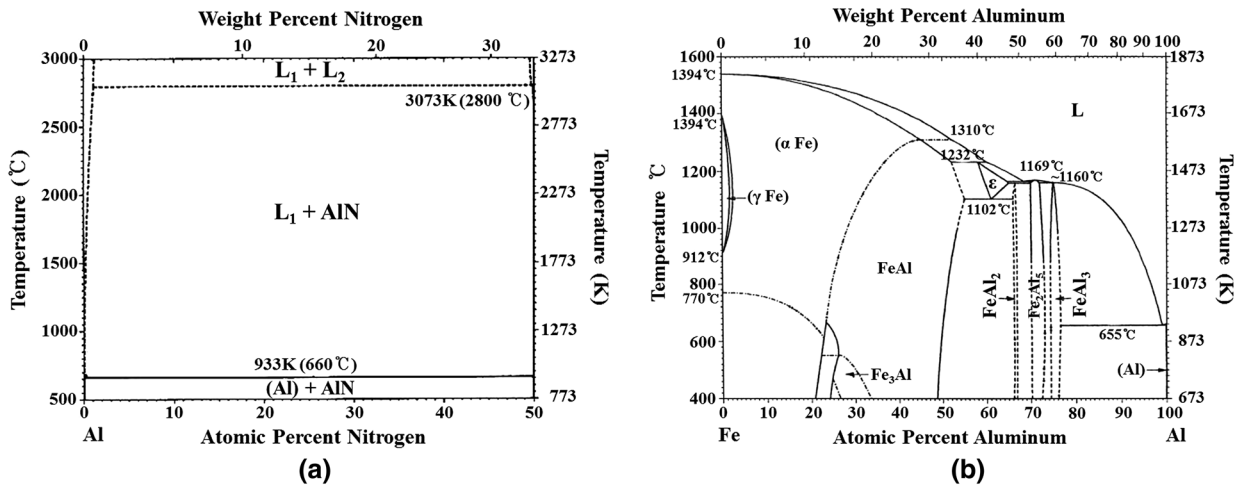
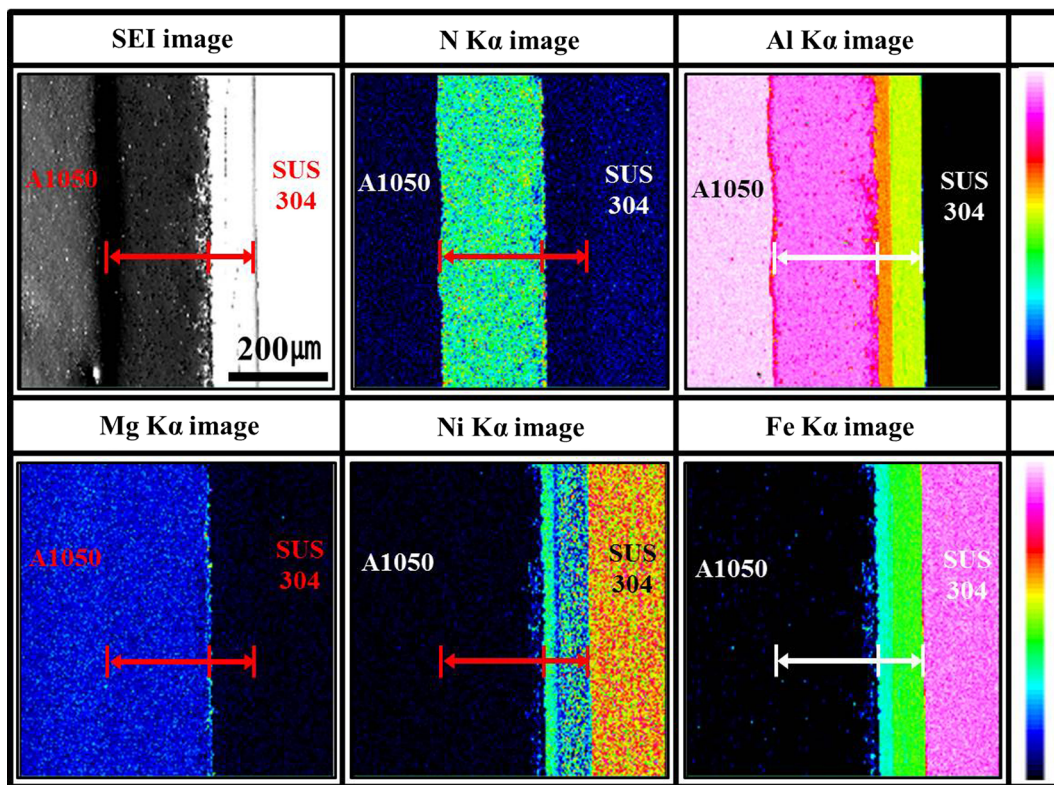Fig. 3—Binary phase diagrams of (*a*) Al-N and (*b*) Fe-Al.

Fig. 4—Characteristic X-ray images of EPMA showing the cross section of bonded layer with barrel nitriding at 893 K (620 °C) for 36 ks.

compound layer. This means that the diffusion of the nitrogen into the aluminum substrate is faster than the diffusion of the aluminum into the steel substrate.

Figure 6 and Table III show the results of the SEM micrographs and EDX analysis on the multilayer after barrel nitriding at 913 K (640 °C) for 36 ks. Using the results of EDX, small amount of oxygen is detected on the Al substrate (Table IIIA). However, the oxygen or some oxides were not detected on the AlN (Table IIIB through D) and Fe-Al intermetallic compound layer (Table IIIE through H) or their interface, because the

oxygen in the furnace reacted with the Al-50 wt pct Mg powder first during the barrel nitriding process. There-fore, it is determined that the amount of oxygen is not enough for forming some oxide at the interface or compound layer. Fe_xAl_y needle-type precipitates are observed at the boundary of the nitride and Fe-Al intermetallic compound layer. From the result of line mapping as shown in Figure 7, the profile of the Al amount is seen to decrease toward the austenitic stainless steel from the pure aluminum substrate. The element of Al, which has a strong affinity with Fe, is
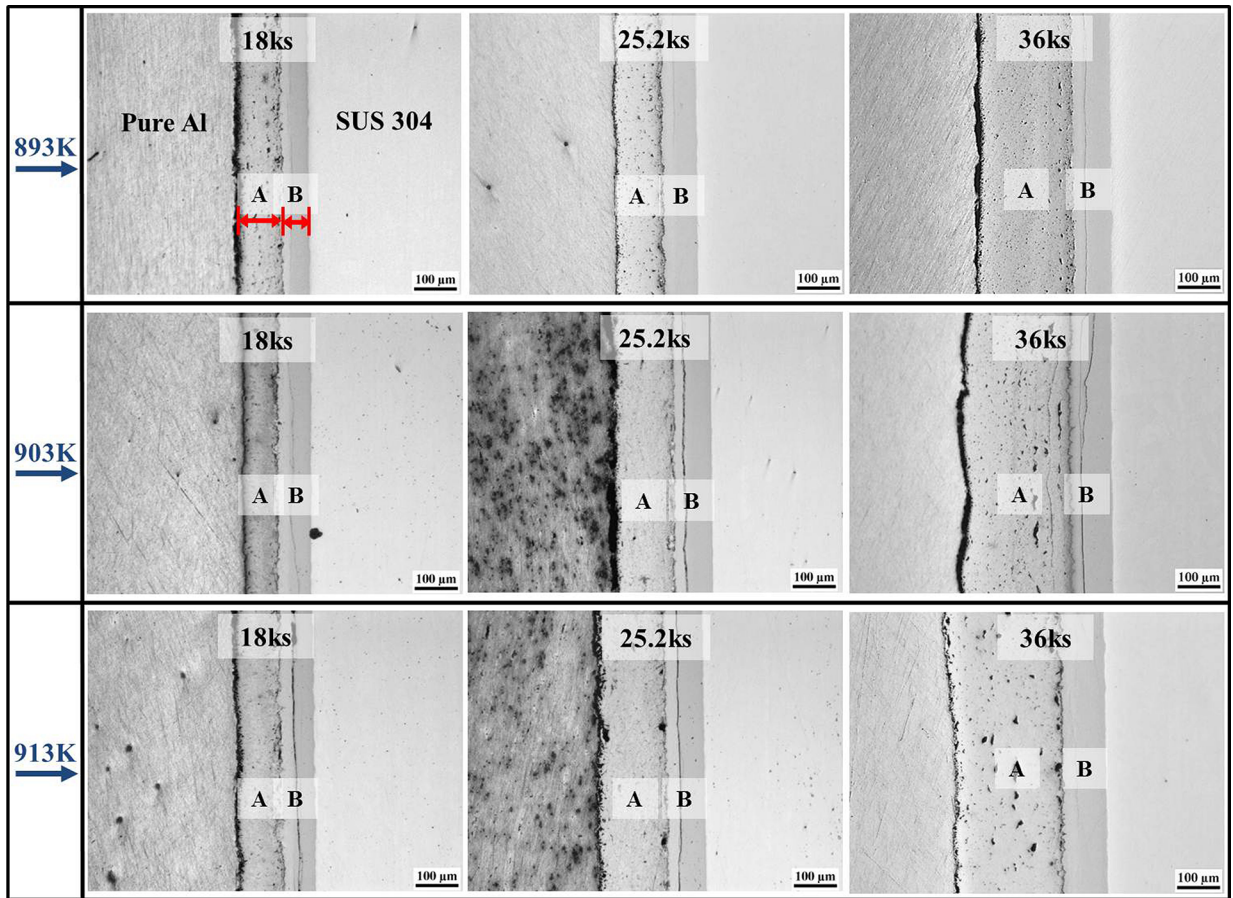
Fig. 5—Cross-sectional micrographs of the multilayer after bonding process at various treatment temperatures and times.
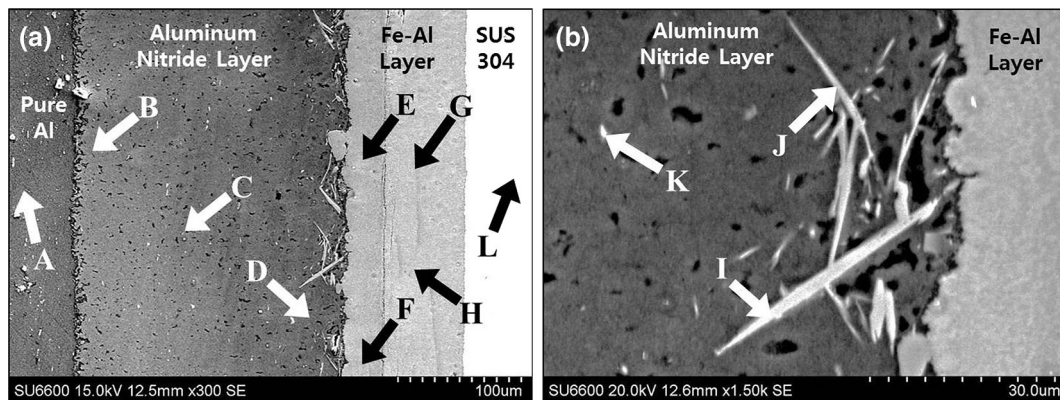

Fig. 6—SEM micrographs of the multilayer after bonding process (barrel nitriding) at 913 K (640 °C) for 36 ks.

thereby diffused to the austenitic stainless steel surface to form the Fe-Al intermetallic layer, while the aluminum nitride layer grows due to the nitrogen permeation into the aluminum side. Therefore, it is expected that the types of Al-rich $FeAl_2$, Fe_2Al_5, or $FeAl_3$ compound exists near the aluminum nitride layer. Additionally, the types of Fe-rich Fe_3Al or FeAl compounds exist near the austenitic stainless steel.

In addition, in the results of the EPMA and EDX, a small amount of the Mg is detected on the nitride layer and the aluminum substrate also. As shown in the phase

diagram of Figure 8, the melting point of the Al-50 wt pct Mg shows about 733 K (460 °C). Therefore, it is believed that the Mg of the Al-50 wt pct Mg alloy powder has penetrated by a capillary phenomenon into the interface between the pure Al and SUS304 stainless steel.

To prove the penetration of the Mg from the Al-50 wt pct Mg alloy powder, the extremely short treatment time of 600 seconds. (holding time) was performed for the bonding process without nitrogen gas. As shown in Figure 9, the island of Al/Mg which has over 10 wt pct Mg is observed at the boundary of pure aluminum and

Table III. EDX Analysis Results After Barrel Nitriding at 913 K (640 °C) for 36 ks

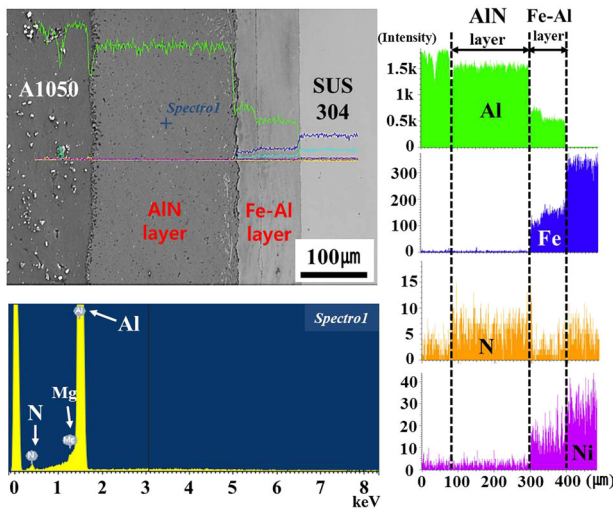| Weight Percent	Al	N	O	Cr	Ni	Si	Mg	Fe
A	97.59	—	2.41	—	—	—	—	—
B	87.79	12.02	—	—	—	—	0.19	—
C	91.00	8.92	—	—	—	—	0.07	—
D	89.67	10.10	—	—	—	—	0.23	—
E	63.42	—	—	5.65	3.68	0.77	—	26.48
F	63.47	—	—	6.84	5.47	0.57	—	23.64
G	52.81	—	—	7.79	9.72	0.09	—	29.59
H	53.33	—	—	8.00	6.34	0.24	—	32.08
I	62.95	0.47	1.61	1.44	4.69	0.07	—	28.76
J	76.77	2.42	—	1.04	2.59	0.18	—	17.00
K	73.49	7.00	—	0.13	0.94	0.07	—	18.37
L	—	—	—	18.87	8.47	0.72	—	70.76
			V(0.13)				Mn(1.06)	

Fig. 7—The profiles of Al and Fe on the aluminum nitride and Fe-Al intermetallic compound multilayer after barrel nitriding at 913 K (640 °C) for 36 ks.
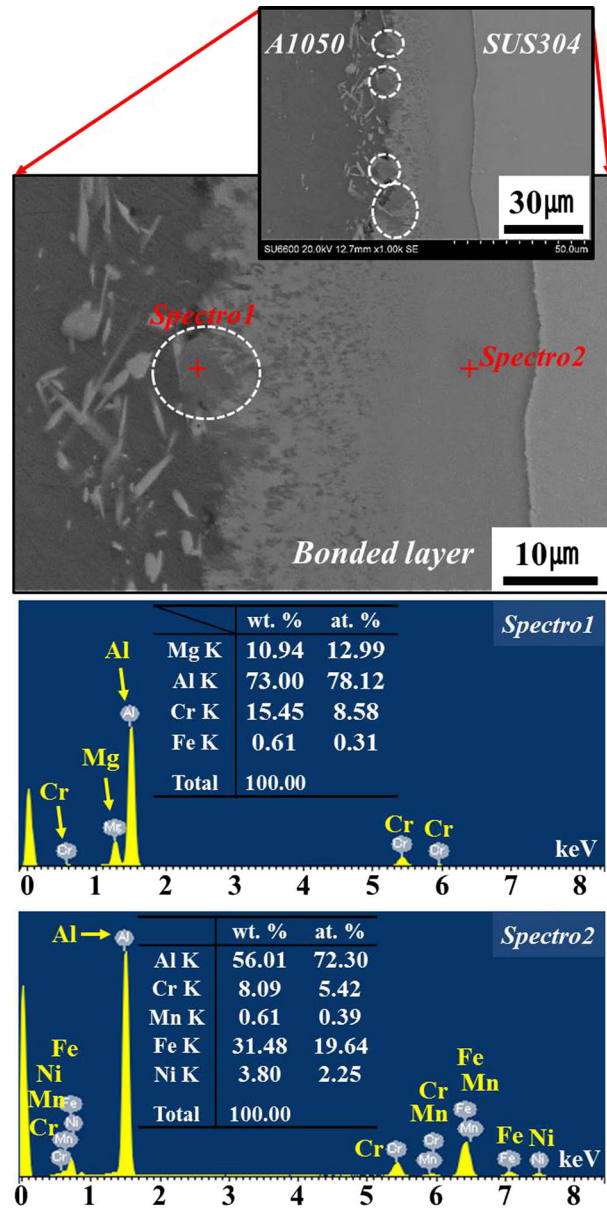

Fig. 8—Al-Mg phase diagram.

Fig. 9—SEM micrographs and EDX results after bonding process at 903 K (630 °C) or 10 min (0.6 ks) without nitrogen gas.
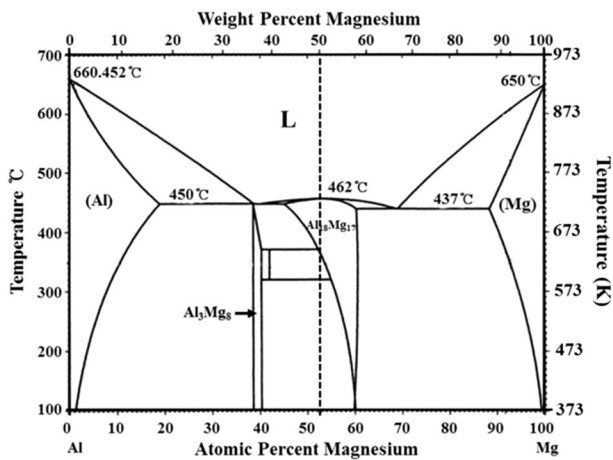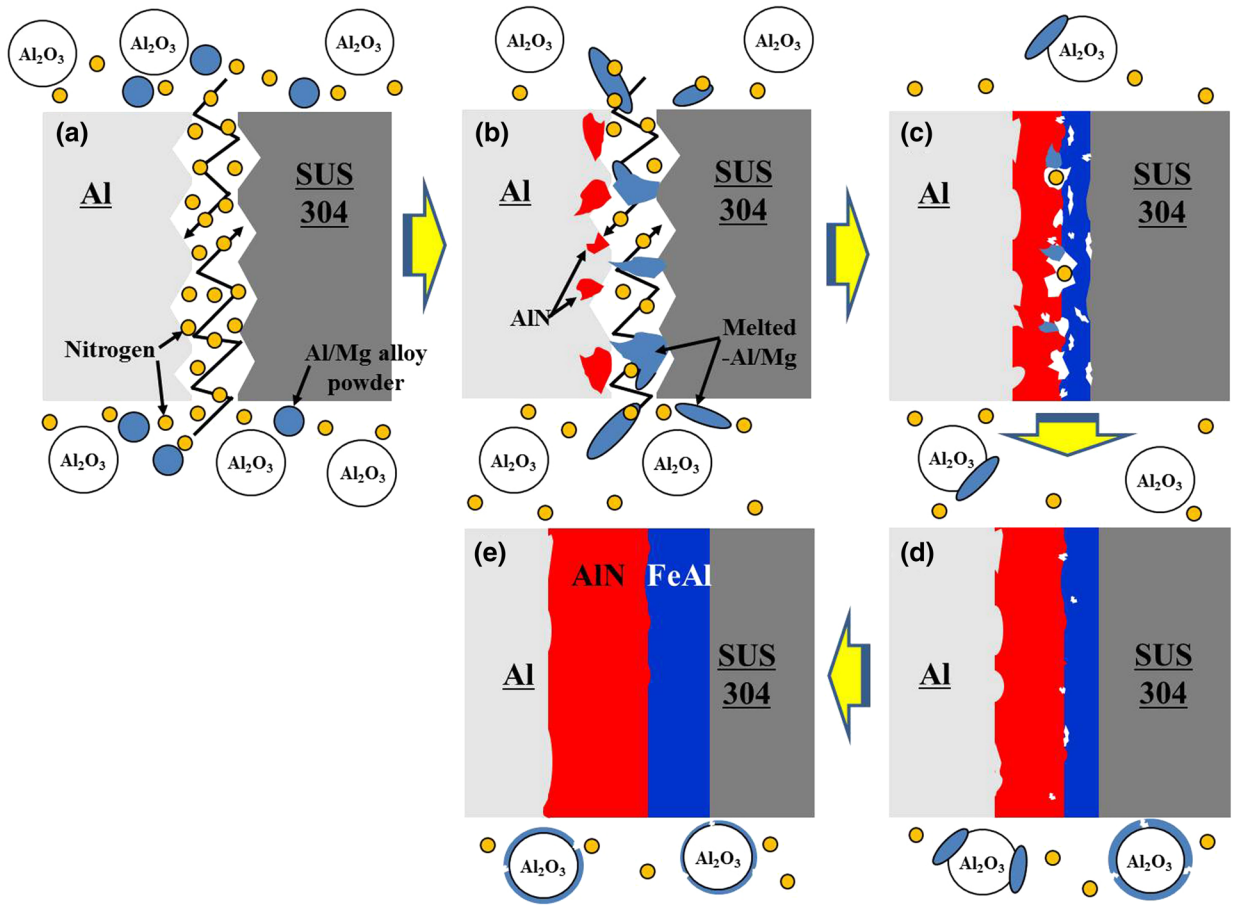
Fig. 10—Schematic illustration of the growth process of aluminum nitride and Fe-Al intermetallic compound layer.
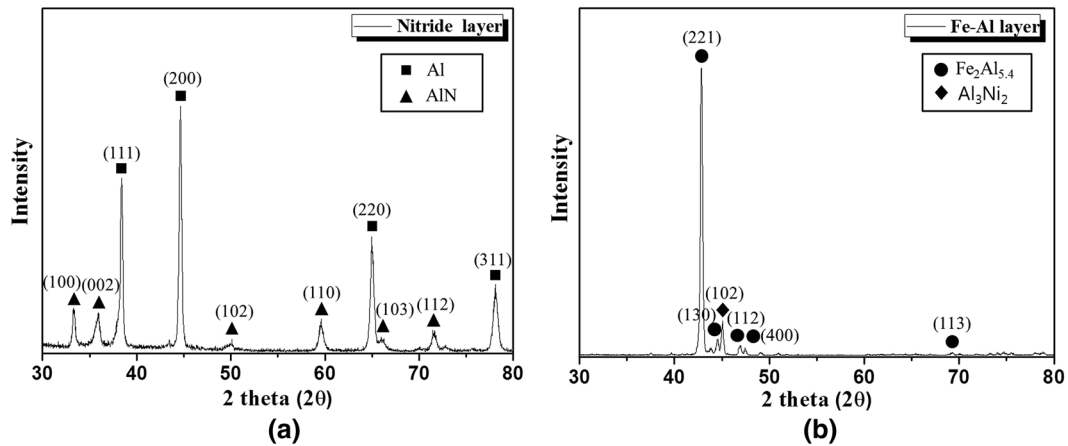

Fig. 11—XRD patterns of the (a) AlN layer and (b) Fe-Al layer after barrel nitriding at 913 K (640 °C) for 36 ks.

Fe-Al intermetallic compound layer. That is, it means that the Mg of the Al-50 wt pct Mg is penetrated into the interface.
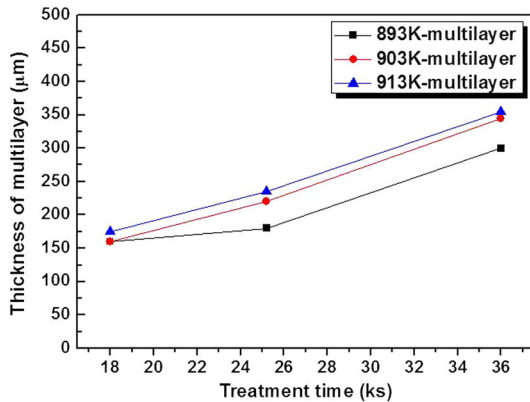
Thus, it is determined that the melted Al/Mg can be reacted with the aluminum substrate at the interface after the melting of alloy powder over 733 K (460 °C), and the molten Al/Mg diffuses into the aluminum substrate with increasing treatment time. Besides, the nitrogen gas can be penetrated more easily into the

interface between aluminum and stainless steel with the molten Al/Mg alloying powder (Figure 10(b)).
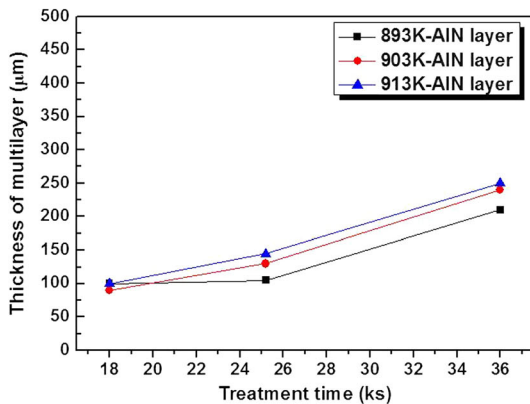
Consequently, the nitrogen can be reacted with the aluminum surface in the interface. At the same time, the Fe-Al intermetallic compound is also formed at the surface of the SUS304 stainless steel (Figure 10(c)). After that, the AlN and Fe-Al intermetallic compound multilayer are uniformly grown by the diffusion of nitrogen and aluminum, respectively (Figures 10(d) and

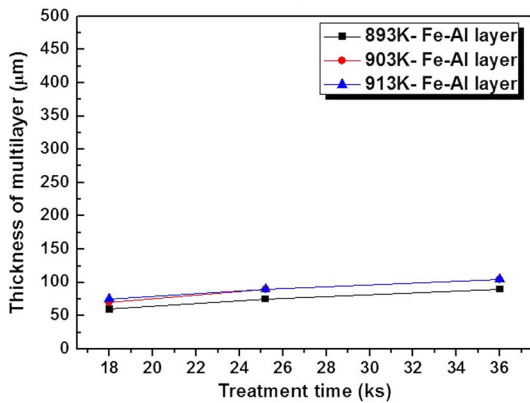(e)). However, it is considered that these processes are very complicated, and take place simultaneously.

To clearly demonstrate that which phases appear at the multilayer between the aluminum and the SUS304 substrate, XRD measurements were performed. Figure 11 (a) and (b) shows the XRD results of the A and B layers after bonding process using the barrel nitriding at 913 K (640 °C) for 36 ks. In the A layer, which is expected to be an aluminum nitride layer, AlN peaks were detected with Al peaks as shown in

Figure 11(a). In the case of the B layer, an intense peak is exhibited which is attributable to (221) $Fe_2Al_{5.4}$ with other low intensity peaks attributable to other Fe compounds, as shown in Figure 11(b). In addition, an Al_3Ni_2 peak is observed due to the diffusion of nickel from the SUS304 substrate on the intermetallic compound layer.

Figure 12 shows the thicknesses of the AlN layer, Fe-Al layer, and the total thickness of the multilayer. As shown in Figures 12(b) and (c), the thicknesses of the AlN and Fe-Al intermetallic layer increased with increasing treatment time and temperature. However, the growth rate of the AlN layer rapidly increased in comparison to the Fe-Al intermetallic compound layer with increasing treatment time and temperature.

Therefore, the total thickness of the multilayer is affected by the thickness of AlN, *i.e.*, the Fe-Al intermetallic compound layer is not significantly changed, as shown in Figure 12(c). Thus, it is determined that the diffusion rate of Al toward the SUS304 is not fast, while the aluminum nitride layer is growing. In addition, it is known that the effect of the treatment time is higher than the effect of the treatment temperature on the growth of the thickness of the multilayer.

To predict the thickness of multilayer at various treatment times, curve fitting was performed. Figure 13 presents the result of curve fitting on the total thickness of multilayer after barrel nitriding at 903 K (630 °C) with various treatment times which range from 10.8 to

Fig. 12—The thicknesses of the (*a*) multilayer, (*b*) AlN layer, and (*c*) Fe-Al intermetallic compound layer at various treatment times after barrel nitriding.
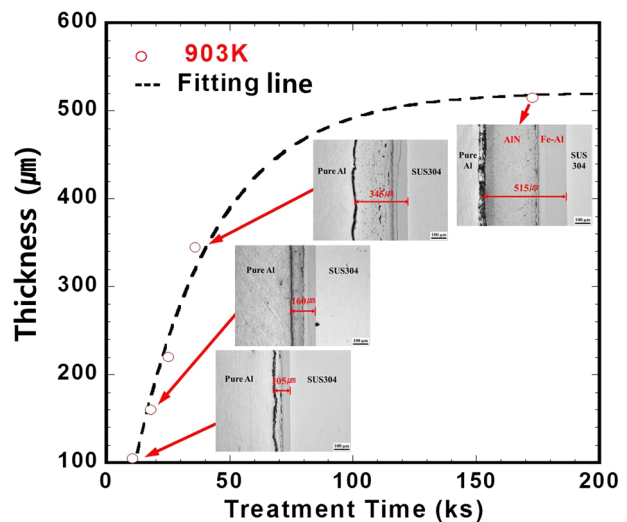

Fig. 13—Curve fitting on the thickness of multilayer at 903 K (630 °C) with various treatment times.

Table IV. Calculation Formula of Fitting Curve

$y = m1 + m2 \times (1 - \exp(-m3 \times x))$	Value
$m1$	−75.485
$m2$	596.4
$m3$	0.030203
R^2	0.98547
R	0.992708

172.8 ks. Computed curve of the figure shows a calculation formula on the thickness of multilayers as shown in Eq. [1].

$$y = m1 + m2 \times (1 - \exp(-m3 \times x)). \qquad [1]$$

That is, the thickness of multilayer can be expected by Eq. [1]. Error for thickness measured by Eq. [1] is under 0.73 pct ($R^2 = 0.98547$). In addition, the values of $m1$, $m2$, and $m3$ are indicated at Table IV.
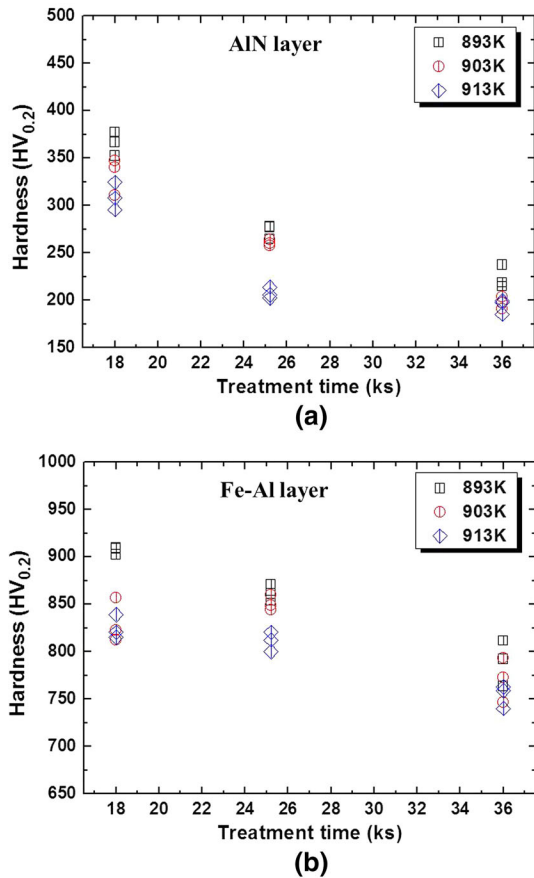

Fig. 14—Average hardness value of (*a*) the AlN layer and (*b*) the Fe-Al intermetallic compound layer, at different treatment times at 893 K, 903 K, and 913 K (620 °C, 630 °C, and 640 °C).

Figure 14 shows the hardness value of the AlN layer and the Fe-Al intermetallic compound layer at different treatment times at each temperature. In general, the area is divided into four types at each specimen: I (pure Al), II (AlN), III (Fe-Al), and IV (SUS304), according to the hardness value.

The hardness values of the pure Al and SUS304 austenitic stainless steel are found to be about 30 HV and 200 HV, respectively. In addition, the maximum hardness of the aluminum nitride layer is found to be 377HV, and the Fe-Al compound layer is found to have a maximum hardness of 910 HV, after bonding process by the barrel nitriding at 893 K (620 °C) for 18 ks. As shown in Figures 14(a) and (b), the hardness values of the AlN and Fe-Al compound layers decreased with increasing treatment temperature. Moreover, the hardness value of the AlN layer shows the range of 377 HV to 290 HV at a treatment time of 18 ks, and the hardness value continuously decreased in the range of 235 HV to 185 HV with increasing treatment time, up to 36 ks. The Fe-Al intermetallic compound layer also shows the range of 910 HV to 815 HV at 18 ks, after that the hardness value decreased to the range of 810 HV to 740 HV when the treatment time was taken to 36 ks at each treatment temperature. That is, the hardness value decreased with increasing treatment temperature and time.

To understand the diffusion behavior of nitrogen and Al at different treatment times and temperatures, the EPMA quantitative analysis was performed on the AlN and Fe-Al intermetallic compound layer. Table V shows the nitrogen and Al concentration on the AlN layer at various treatment temperatures and times (⟨893 K, 18 ks⟩, ⟨893 K, 36 ks⟩, and ⟨903 K, 36 ks⟩). As shown in Table V, the nitrogen concentration on the AlN layer shows about 24 wt pct at the 893 K (620 °C), 18 ks. After that, the average concentration of nitrogen decreased with increasing the treatment time and temperature. That is, the diffusion of nitrogen at the AlN layer is continuously maintained, and the thickness is continuously increased. However, the concentration of nitrogen is gradually decreased when takes longer treatment time, because it is expected that the nitrogen could not be supplied into the narrow interface between the aluminum and SUS304 stainless steel after the AlN and Fe-Al thin layer is formed completely. Thus, it is expected that the number of nitrogen atoms is very

Table V. The EPMA Quantitative Analysis Result of Al and Nitrogen on the AlN Layer

	893 K (620 °C), 18 ks		893 K (620 °C), 36 ks		903 K (630 °C), 36 ks	
	AlN Layer		AlN Layer		AlN Layer	
	Al (Wt Pct)	N (Wt Pct)	Al (Wt Pct)	N (Wt Pct)	Al (Wt Pct)	N (Wt Pct)
1st	70.8855	28.4930	78.0617	21.6898	80.7633	19.0374
2nd	75.8348	23.7365	78.2924	21.4207	81.2738	18.3607
3rd	76.1992	23.3871	78.0914	21.6609	81.5862	18.1229
4th	76.5156	23.1356	80.1808	19.5242	80.1356	19.5280
5th	74.4977	25.1262	80.9513	18.8061	82.2377	17.5330
Average (wt pct)	74.7866	24.7757	79.1155	20.6203	81.1993	18.5164

Table VI.   The EPMA Quantitative Analysis Result of Fe and Al on the AlN Layer

| | 893 K (620 °C), 18 ks | | 893 K (620 °C), 36 ks | | 903 K (630 °C), 36 ks | |
| | Fe-Al Layer | | Fe-Al Layer | | Fe-Al Layer | |
	Fe (Wt Pct)	Al (Wt Pct)	Fe (Wt Pct)	Al (Wt Pct)	Fe (Wt Pct)	Al (Wt Pct)
1st	23.3163	65.6292	33.1207	56.8283	35.0801	56.4608
2nd	25.7474	65.3570	33.0084	56.9910	27.6135	54.3636
3rd	23.9131	66.0589	35.0690	56.4669	35.2184	55.8850
4th	29.3138	63.8253	33.1389	56.6705	34.9445	56.5295
5th	23.8921	65.4241	26.3453	55.2449	33.7303	55.5138
Average (wt pct)	25.2365	65.2589	32.1365	56.4403	33.3173	55.7505

important when nitrogen is beginning to permeate into the aluminum surface of the interface. And, the changes of nitrogen concentration at various treatment temperatures and times showed similar tendency with the hardness variation of AlN layer. In case of Fe-Al intermetallic compound layer, the Al concentration is decreased with increasing the treatment temperature and time as shown in Table VI. On the other hand, the concentration of Fe is gradually increased with increasing the temperature and time. Therefore, it is determined that the hardness of Fe-Al intermetallic compound layer is decreased with increasing the Fe concentration and decreasing the Al concentration.

IV.   CONCLUSIONS

The aluminum nitride layer and the Fe-Al intermetallic compound layer formed between the pure aluminum and the SUS304 austenitic stainless steel after the bonding process by barrel nitriding at 893 K, 903 K, and 913 K (620 °C, 630 °C, and 640 °C) for treatment time of 10.8, 18, 25.2, 36, and 172.8 ks. The results obtained are as follows:

1. As ascertained from the XRD analysis, the multilayer is composed of an AlN layer and a $Fe_2Al_{5.4}$ intermetallic compound layer.
2. The total thicknesses of the multilayer are found to be 160, 180, and 300 μm at 893 K (620 °C) for treatment times of 18 ks, 25.2 ks, and 36 ks, respectively. In addition, the thicknesses of the AlN and Fe-Al intermetallic compound layers increased with increasing treatment time and temperature.
3. Fitting curve as basis on the thickness of multilayer at 903 K (630 °C) shows a calculation formula on the thickness of multilayers as shown in Eq. [1]. From this equation, it is possible to expect the thickness of multilayer at 903 K (630 °C) for various treatment times.

$$y = m1 + m2 \times (1 - \exp(-m3 \times x)). \qquad [1]$$

4. The maximum hardness of the aluminum nitride layer was found to be 377 HV, and the Fe-Al compound layer showed a maximum hardness of 910 HV, after barrel nitriding at 893 K (620 °C) for 18 ks. Additionally, the hardness value decreased with increasing treatment temperature and time.

REFERENCES

1. S. Tomida and K. Nakata: *Surf. Coat. Technol.*, 2003, vols. 174–175, pp. 559–63.
2. M. Okumiya, Y. Tsunekawa, H. Sugiyama, Y. Tanaka, N. Takano, and M. Tomimoto: *Surf. Coat. Technol.*, 2005, vol. 200, pp. 35–39.
3. I.N. Fridlyander, V.G. Sister, O.E. Grushko, V.V. Berstenev, L.M. Sheveleva, and L.A. Ivanova: *Met. Sci. Heat Treat.*, 2002, vol. 44, pp. 365–70.
4. F. Ostermann: *Mater. Sci. Eng. A*, 1995, vol. 199, pp. 73–77.
5. S. Kobayashi and T. Yakou: *Mater. Sci. Eng. A*, 2002, vol. 338, pp. 44–53.
6. E. Taban, J.E. Gould, and J.C. Lippold: *Mater. Sci. Eng. A*, 2010, vol. 527, pp. 1704–08.
7. E. Taban, J.E. Gould, and J.C. Lippold: *Mater. Des.*, 2010, vol. 31, pp. 2305–11.
8. M.J. Rathod and M. Kutsuna: *Weld. J.*, 2004, vol. 83, pp. 16–26.
9. T. Tanaka, T. Morishige, and T. Hirata: *Scripta Mater.*, 2009, vol. 61, pp. 756–59.
10. W.B. Lee, M. Schmuecker, U.A. Mercardo, and G. Biallas: *Scripta Mater.*, 2006, vol. 55, pp. 355–58.
11. M.S.A. Nezhad and A.H. Ardakani: *Mater. Des.*, 2009, vol. 30, pp. 1103–09.
12. J. Tsujino, K. Hidai, A. Hasegawa, R. Kanai, H. Matsuura, K. Matsushima, and T. Ueoka: *Ultrasonics*, 2002, vol. 40, pp. 371–74.
13. J. Tsujino, T. Ueoka, T. Kashino, and F. Sugahara: *Jpn. J. Appl. Phys.*, 1999, vol. 38, pp. 4254–55.
14. T. Aizawa, M. Kashani, and K. Okagawa: *Weld. J.*, 2007, vol. 86, pp. 119–24.
15. M. Okumiya, M. Yoshida, R. Ichiki, C. Tekmen, W. Khalifa, Y. Tsunekawa, and K. Tanaka: *Plasma Process. Polym.*, 2009, vol. 6, pp. 287–90.
16. J.H. Kong, M. Okumiya, Y. Tsunekawa, S.G. Kim, and M. Yoshida: *Prog. Org. Coat.*, 2013, vol. 76, pp. 1841–45.
17. F.D. Lai: *J. Vac. Sci. Technol.*, 2004, vol. 22B, pp. 1174–78.
18. T.J. Mroz, Jr.: *Ceram. Bull.*, 1992, vol. 71, pp. 782–84.
19. S. Gredelj, A.R. Gerson, S. Kumar, and G.P. Cavallaro: *Appl. Surf. Sci.*, 2002, vol. 199, pp. 183–94.
20. F.-X. Liu, B.-Y. Huang, K.-C. Zhou, Y. Liu, and J.-X. Chen: *Mater. Sci. Eng. Powder Metall.*, 2000, vol. 5, pp. 193–200.

21. S.D. Deevi, M.R. Hajaligol, A. Cliff Lilly, and G.S. Fleischhauer: *Trans. Nonferrous Met. Soc. China*, 1999, vol. 9, pp. 309–17.
22. X. Zhu, Z. Yao, X. Gu, W. Cong, and P. Zhang: *Trans. Nonferrous Met. Soc. China*, 2009, vol. 19, pp. 143–48.
23. E.I. Meletis and S. Yan: *J. Vac. Sci. Technol. A*, 1991, vol. 9, pp. 2279–84.
24. B. Kurt, N. Orhan, E. Evin, and A. Calik: *Mater. Lett.*, 2007, vol. 61, pp. 1747–50.
25. Y.S. Han, K.B. Kalmykov, S.F. Dunaev, and A.I. Zaitsev: *J. Phase Equilib. Diffus.*, 2004, vol. 25, pp. 427–36.
26. U.R. Kattner and T.B. Massalski: in *Binary Alloy Phase Diagrams*, H. Baker, ed., ASM International, Material Park, OH, 1990, p. 147.